

Multistatic Radar Classification of Armed vs Unarmed Personnel Using Neural Networks

Jarez Patel¹, Francesco Fioranelli² Matthew Ritchie¹, and Hugh Griffiths¹

¹ University College London, Torrington Place, WC1E 7JE, London

[jarez.patel.13,m.ritchie,h.griffiths@ucl.ac.uk,

² University of Glasgow, University Avenue, G12 8QQ, Glasgow

Francesco.Fioranelli@glasgow.ac.uk

Abstract. This paper investigates an implementation of an array of distributed neural networks, operating together to classify between unarmed and potentially armed personnel in areas under surveillance using ground based radar. Experimental data collected by the University College London (UCL) multistatic radar system NetRAD is analysed. Neural networks were introduced to the extracted micro-Doppler data in order to classify between the two scenarios, and accuracy above 98% is demonstrated on the validation data, showing an improvement over methodologies based on classifiers, where human intervention is required. The main advantage of using neural networks is to bypass the manual extraction process of handcrafted features from the radar data, where thresholds and parameters need to be tuned by human operators. Different network architectures are explored, from feed-forward networks to stacked auto-encoders, with the advantages of deep topologies being capable of classifying the spectrograms (Doppler-time patterns) directly. Significant parameters concerning the actual deployment of the networks are also investigated, for example the dwell time (i.e. how long the radar needs to stare at a target in order to achieve classification), and the robustness of the networks in classifying data from new people, whose signatures were unseen during the training stage. Finally, a data ensembling technique is also presented which utilises a weighted decision approach, established beforehand, utilising information from all three sensors, and yielding stable classification accuracies of 99% or more, across all monitored zones.

Keywords: Multistatic Radar, Classification, Deep Neural Networks, Auto-Encoders, Micro-Doppler, Data Ensembling

1 Acknowledgements

This work has been funded by the IET A. F. Harvey Prize awarded to Hugh Griffiths (2013), and by the UK Engineering and Physical Sciences Research Council (EPSRC) which funded Jarez Patel for his internship (2015).

2 Introduction

Micro-Doppler signatures in radar are generated from additional modulations on top of the main Doppler shift of a moving target and are related to moving, vibrating or rotating parts. People exhibit these signatures as they are associated with the motion of the limbs and body, and these have been studied and characterised for a variety of applications (Youngwook & Hao, 2009; Chen, Tahmoush & Miceli, 2014). Human micro-Doppler has been used by radar to discriminate between different activities such as running, crawling, or walking (Youngwook & Hao, 2008), to identify humans rather than animals such as horses or dogs, or vehicles (Youngwook, Sungjae & Jihoon, 2015), and even to distinguish between men and women (Tahmoush & Silvious, 2009). The characterisation of free or confined movements of the arms utilising micro-Doppler analysis has also been reported (Fioranelli, Ritchie & Griffiths, 2015; Tivive, Bouzerdoum & Amin, 2010), whereby limited movement can be related to the presence of hostages, injured people or the carrying of potential hostile objects (given the implementation in the appropriate environment).

The micro-Doppler signature produced by a human target has been shown to be strongly dependent on the aspect angle and the geometry of the radar system (Fioranelli et al., 2015). Bistatic and multistatic radar systems propose to mitigate this issue, as multiple radar sensors can be deployed to provide a multi-perspective view on the target, with at least one subset of sensors illuminating the scene from a favourable angle.

The main contribution of this study is an investigation into the potential of neural networks to improve the classification performance of radar processing, in this specific case for identifying armed vs un-armed personnel which expands upon previous research (Fioranelli et al., 2015). Different network architectures are considered, namely feed-forward networks, stacked auto-encoders and altogether a deep network. One of the advantages is the possibility of bypassing the extraction of handcrafted features specified and chosen by the human operator. Some of these features have shown to be effective (Fioranelli et al., 2015), but there is always a risk of discarding relevant information when implementing feature extraction, and the actual implementation often requires setting and tuning various parameters and thresholds, which severely limit the possibility to apply the chosen method to new datasets and new subjects. With auto-encoders and deep topologies (Haykin, 2008), (LeCun, Bengio & Hinton 2015), the radar micro-Doppler signatures, i.e. the Doppler vs. time images, are considered directly as raw data input, leaving to the network itself the task of selecting the important information for classification purposes. In addition to this, different ways of combining information from multiple, spatially distributed radar nodes together with neural network processing are investigated, leveraging real experimental data collected using a multistatic radar available at University College London (Derham, 2007).

There is some existing work in using neural networks for classification based on human micro-Doppler radar data. In (Youngwook & Moon, 2016) the authors tested two different convolutional networks with 2 and 3 convolutional layers to classify human vs. animals and vehicles, and to discriminate between 7 different indoor activities performed by 12 subjects, respectively. The average accuracy was approximately 90% for the activity classification. The effect of different dwell times was also briefly observed. Convolutional neural networks were also exploited in (Parashar et al., 2017) for identification of target classes in the context of automotive radar, for example pedestrians and bicycles vs cars and vehicles, and in (Seyfoglou, 2017) to discriminate different human actions and activities in the context of ambient assisted living and remote health monitoring. In both cases, the micro-Doppler signatures were used directly as inputs to the network. Furthermore, convolutional networks were also used in (Park et al., 2016) to classify between different types of swimming styles for aquatic human targets, and in (Youngwook & Toomajian, 2016) to classify between different hand gestures in the domain of human-machine interaction and usage of smart devices. In (Kwon & Kwak, 2017) a feed-forward neural network was used to detect the presence of humans in outdoor or indoor areas of interest, against background interference given by natural phenomena such as rain or manmade items such as rotating fans. In (Jordan, 2016) the author used DCNNs to approach three classification problems, one of which was the classification of the indoor activities in the same dataset also analysed in (Youngwook & Moon, 2016). The authors initially trained and tested the network on data from different people to validate its capabilities of generalizing the performance to new data, but only 82.7% accuracy was reported. This was improved to 93.4% when data from all available subjects were used for both training and testing. In (Jokanovic, Amin & Amad 2016) a neural network consisting of stacked auto-encoders and a softmax classifier was used to discriminate between 4 activities, taking care of performing the movements at normal and fast speed. This paper reported good accuracy at 87%, but the number of subjects taking part in the experiment was not specified, as well as whether the network was trained and tested on data from different people or not. The same authors used a similar network architecture based on stacked auto-encoders plus softmax to investigate the use of different time-frequency distributions generating the micro-Doppler images to use as inputs to the network (Jokanovic, Amin & Amad 2016), and to explore the effect of different data representations (i.e. range-time, range-Doppler, time-Doppler) (Jokanovic, Amin & Amad 2017).

These previous works borrowed a single network architecture from existing research in the computer science and pattern recognition domains for the analysis of radar data. The investigation presented in this paper aims to perform a comparison of different network architectures, starting from the simplest case of feed-forward network using handcrafted features, to a deep network operating directly on the raw spectrograms. An important element is the use of experimental data from the distributed nodes of the UCL multistatic radar system,

as there are few such data analysed in the open literature, and, to the best of the authors knowledge, the existing work on neural networks for classification of radar data has so far only taken into account monostatic data. Furthermore, the investigation of parameters that are relevant to the actual deployment in the field of the system, such as the dwell time, the relative position of the target in different zones with respect to the radar nodes, and the combination of information from multiple radar nodes is also presented in this paper. These are important parameters, whose effect on the overall classification accuracy of the proposed system has to be characterised for an effective deployment and use.

The rest of the paper is organised as follows: section 3 will cover the theory behind the Doppler effect exhibited in radar, section 4 will detail the specifications of the radar system (NetRAD) including the experimental setup. Section 5 presents the data analysis processes involved; section 6 will provide the results of the analysis and section 7 will conclude the paper, including areas for future work.

3 Theory

In a coherent pulsed radar which is frequency modulated, the frequency offset in the return signal caused by the Doppler effect, with respect to a dynamic target in a monostatic environment is represented by Equation 1, where f_c is the carrier frequency of the radar and θ is the angle between the velocity component v of the target and the Line of Sight (LoS) of the radar (Stimson et al., 2014).

$$f_d = \frac{2f_c v}{c} \cos(\theta) \quad (1)$$

In a bistatic radar system, the equation must be modified to account for the differing angle between the transmitter and the receiver, this is given by β within Equation 2. The angle δ represents the angle between the bistatic LoS and the velocity vector of the target.

$$f_d = \frac{2f_c v}{c} \cos\left(\frac{\beta}{2}\right) \cos(\delta) \quad (2)$$

In addition to these Doppler components further modulation is exhibited, known as micro Doppler, these are superimposed onto the main Doppler offset and convey further information regarding the finer movements of the target. With this work focusing on the movements of the arms and legs (limbs) of a human target and exploiting this effect to reveal behavioural information, however this is not specifically restricted to humans and can be observed on any target which is moving which contains further moving components, such as an aircraft or helicopter.

4 Radar System & Experimental Setup

The multistatic radar system NetRAD was used to collect the data presented in this paper. NetRAD is a coherent pulsed radar system with three separate but identical radar nodes operating at S-band (2.4 GHz), transmitting with a power of 23 dBm, over a bandwidth of 45 MHz (Derham, Doughty, Woodbridge & Baker, 2007; Doughty 2007). The antennas used have a beam width of approximately $10^\circ \times 10^\circ$ allowing each zone out in the field to be engulfed by the beam. The recording time was 5 s in order to capture several periods of the average human walking gait and the PRF was set to 5 KHz to improve Doppler resolution in the frequency domain.

The experiment was performed in a large open field at the UCL sports ground in Shenley on July 2015, with the setup employing three radar sensors along a linear baseline with 50 m inter-nodal separation. Node 1 was the transceiver, and Nodes 2 and 3 were the passive receive only nodes. As the transmitted beam is narrow, all the antennas were focused at the centre of each zone for each subsequent test. The subjects taking part in the experiment all took turns walking in each of the different zones located in front of the radar system towards the linear baseline, this is shown in Figure 4. Data was collected from each person walking in each zone, generating 360 samples overall: 2 people, 3 nodes, 6 zones, and 10 repetitions per person, i.e. 5 ‘unarmed’ or free handed and 5 ‘armed’, where the target was carrying a metallic pole of 1 m in length, mimicking the constrained movement of holding a rifle.

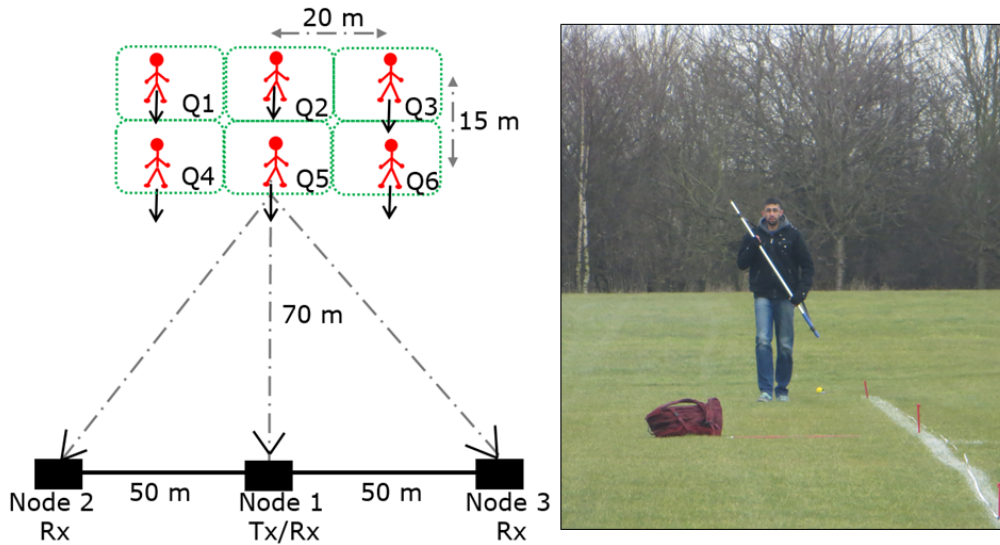


Fig. 1. Experimental Configuration

5 Data Analysis

The samples were collected from the three radar nodes post-trial and were processed; this consisted of match filtering the data, whereby the received signal is correlated with the known transmitted signal gathered from a prior calibration stage. This process allows inaccuracies to be dealt with and as a consequence (amongst others) the quality of the received signal is also significantly improved; this is commonly referred to as the signal to noise ratio (SNR) (Stimson et al., 2014). This produces a range time intensity plot (RTI) as shown in Figure 2, where the pulse number is on the y axis representing time, the range is on the x axis shown in meters and the intensity of the radar return is represented as a colour increasing from blue to red. The range resolution of the radar system is approximately 3 m. This is an RTI collected from Node 1 at Zone 1 which was the monostatic transceiver, hence there is an intense red line at 0 range which was caused by the transmitter being beside the receiver. The target is located between ranges 81 m and 75 m, this indicates that the target walked from a distance of approximately 6 m towards Node 1.

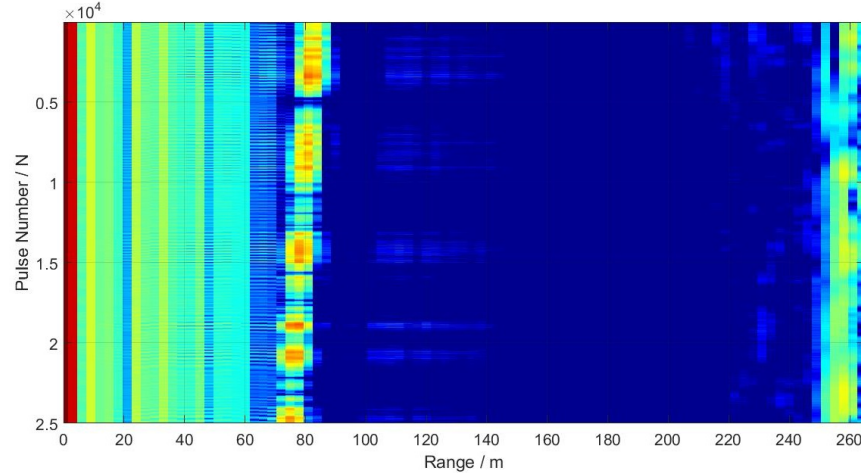


Fig. 2. Radar Range-Time-Intensity Plot for a person walking towards the radar

Once the location of the target is identified a Short Time Fourier Transform (STFT) is then performed over this location with a window length of 0.3s and a 95% overlap factor to generate the respective spectrogram, revealing the frequency (Doppler and micro-Doppler) properties of the target with respect to time; this is computed by evaluating Equation 3 (Fioranelli et al., 2015). The spectrograms provide a deep insight into the movement of the target; the swinging of the arms correspond to micro-Doppler ‘tails’ and the movement of the torso is related to the red main-Doppler signature at the centre, as shown in Figure 3.

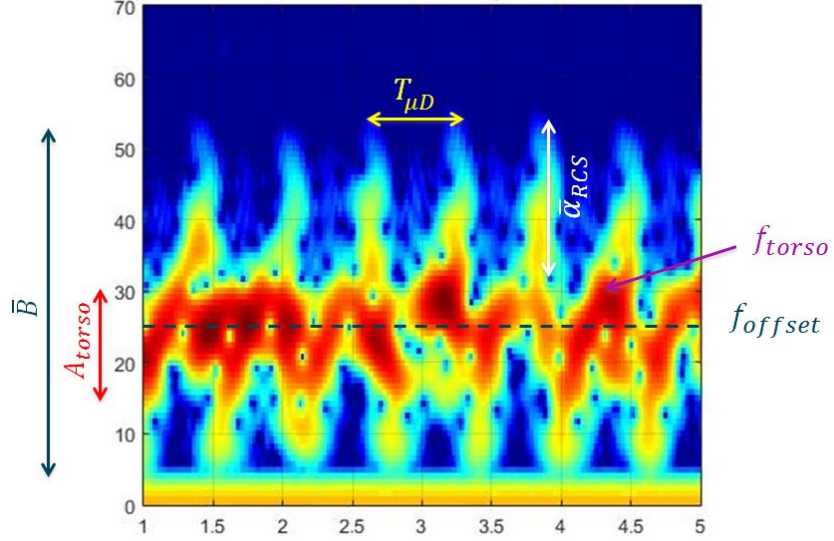


Fig. 3. Spectrogram with micro-Doppler signature of a person walking and labelled features

$$X(M, w) = \left| \sum_{n=-\infty}^{\infty} x[n]w[n-m]e^{-j2\pi f_n} \right| \quad (3)$$

Several empirical features related to physical characteristics of the target and their motions were investigated. These were: Doppler offset (related to the main Doppler component), bandwidth (the difference between the micro and the main Doppler constituents), amplitude (of the main Doppler), period (time difference between two successive micro Doppler peaks), RCS ratio (logarithmic ratio between the micro Doppler to the main), Doppler frequency (of the main Doppler component) and target velocity. This is shown pictorially in Figure 3 and collectively in Matrix 4. From these 7 features, 3 were selected and extracted as the most beneficial for the unarmed vs armed discrimination analysis presented, these were bandwidth, amplitude and RCS ratio (Fioranelli et al., 2015).

$$Y = [f_{Torso}, A_{Torso}, \bar{B}, \bar{\alpha}_{RCS}, f_{Offset}, t_{\mu D}] \quad (4)$$

A simple feature extraction algorithm was developed to quantify these characteristic features, it worked by applying edge detection of the form gradient magnitude coupled with manual thresholding techniques to obtain the vectors of interest. This algorithm relied on human intervention to set the threshold levels by visual inspection making it unequipped for dealing with different data sets. These were then analysed by in some cases evaluating Equations 1 and 2 and decomposing them into singular values, finally these were collected in Matrix 4 for each spectrogram yielding the sample.

5.1 Two Layer Feed-Forward Neural Network

Individual neural networks (NN) of a two layer feed forward architecture containing 30 neurons in the hidden layer and 2 neurons at the output were trained on 60% of the data gathered from both the zone and the node. Since these recordings have a dwell time of 5 s, these were split into two 2.5 s sets to increase the total number of samples to 40. The feature extraction algorithm then processed all the spectrograms generating a database of features, these were then used to train the NN which were then stored as objects and organised with respect to the node and zone they belong to, this results in a 6 by 3 matrix: $\mathbf{N}_{N,Z}$.

Further to this, 20% of the data was applied to this network to generate $\mathbf{Y}_{N,Z}$, which is a matrix that represents the classification accuracy of the network under test and is used to synthesise the weighting matrix[†] which is utilised in the latter combined decision stage. The remaining 20% of the data is reserved solely for testing purposes.

5.2 Classification Ensembling

There are many methods in which a decision algorithm can be implemented in a data orientated system, such as; binary decision tree's, voting or even fuzzy logic. In this work a weighted decision approach was taken whereby each of the generated neural networks were allocated a unique weight (unit-less) which is strongly related to the performance of the individual network in response to the pre-allocated test data (20% share). The weighting matrix is derived through directly mapping a matrix of results $\mathbf{Y}_{N,Z}$ onto an exponential function tending to 100% accuracy, this is given by the weighting matrix $\mathbf{W}_{N,Z}$.

$$\mathbf{W}_{N,Z} = \frac{\alpha \mathbf{Y}_{N,Z}}{100.1 - \mathbf{Y}_{N,Z}} \quad (5)$$

Mapping the accuracy onto a non-linear function allows neural networks which achieved high classification rates to be favoured much more than ones which did not. The value assigned to alpha enables the steepness of the curve to be tuned enabling networks with very similar performances in the same zone to have either more or less influence in the final decision. The value of alpha which yielded good performance was found to be 3, it should be noted that this value is completely dependent on the input matrix $\mathbf{Y}_{N,Z}$ and it should ideally be optimised over a much larger dataset to give it statistical significance.

To differentiate between the two classes when the network makes a prediction, the armed cases are assigned a negative value of 1, whilst the unarmed cases are assigned a positive 1, represented by $\mathbf{P}_{N,Z}$. This allows the decision of that node to constructively or destructively interfere with the others; shown in Equation 6, where the dot product is taken over the weighting matrix and the predicted

[†] The weighting matrix is not related to the weighting function computed by the neural network.

values across the three nodes in the radar system. As a consequence of this operation, it is only necessary to evaluate the sign of the D_Z which reveals what the three nodes believe is the nature of the target in that particular zone in the field.

$$D_Z = W_{1,Z} \cdot P_{1,Z} + W_{2,Z} \cdot P_{2,Z} + W_{3,Z} \cdot P_{3,Z} \quad (6)$$

5.3 Stacked Auto-Encoders

To utilise the full capabilities of neural networks the possibility of classifying on only the spectrograms was investigated, in this case each spectrogram was treated as an input matrix of pixels. An appropriate compromise was made between processing feasibility and quality of results, a good candidate to meet these needs was the auto-encoder. In addition to this, stacking auto-encoders could alleviate strain on processing and also increase performance as each layer of representation would not be forced to become too complex during the supervised learning phases.

The architecture of this neural network consists of multiple stacked auto-encoders employing a sigmoid activation function, followed by a softmax regression layer which together forms a deep neural network (DNN); a diagram of this configuration is shown in Figure 4. The first layer is the input, which is followed by a hidden layer consisting of 1000, 500, 100 and 20 neurons respectively; finally the softmax layer is reached consisting of 2 neurons. The layering allows each stage to learn a progressively compressed representation of the given input vector (Haykin, 2008). The input is a 7800 element matrix for a 5 s spectrogram split into 4; as it propagates through the network the dimensionality of the spectrogram is reduced until it ultimately becomes a two dimensional matrix representing the case of either armed or unarmed.

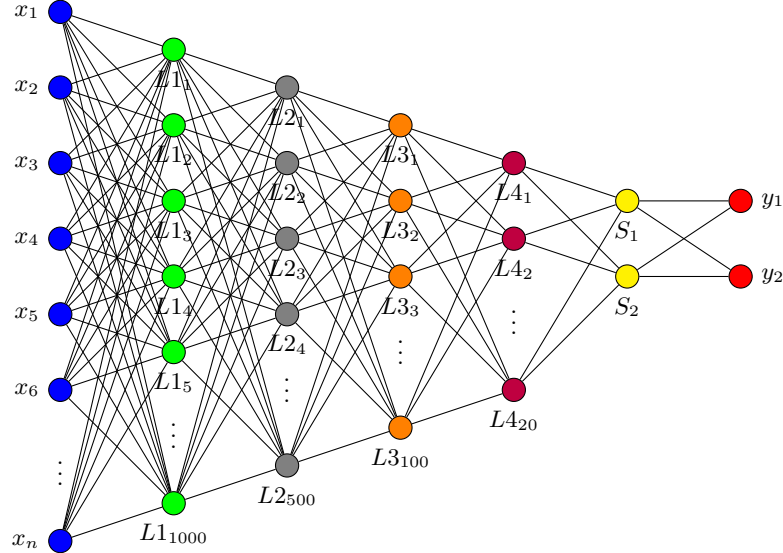


Fig. 4. Architecture of Deep Topology Implemented

6 Results

In this section the results of applying the allocated testing data to the systems described above are presented, firstly testing on the feature based two layer feed-forward neural network and then secondly the performance characteristics of the proposed configuration using the stacked auto-encoder, followed by comparative tests which test the integrity and also the benefits each design.

6.1 Feature Based Neural Networks

Before the data set is applied to the feed-forward neural network, they are firstly separated into the two cases of armed and unarmed, randomised and then stored into the desired group sizes (40 samples total) (60% training, 20% testing and 20% validation); this is done for each zone and each node. Separating the two cases, shuffling and then recombining ensures that the trained network has a clear and unbiased understanding of both classes before data is presented, this in particular is an issue when a small number of samples are available.

The neural network is then trained and tested with the allocated groups of data over 200 Monte Carlo simulations, with the results of the non-cooperative decision (reference data) testing on both the testing and the validation data (40% share in total), the results of which are detailed under the score column (S) of Table 1. The testing data (20%) is then applied generating $\mathbf{Y}_{N,Z}$, which is then transformed into $\mathbf{W}_{N,Z}$ given by the weighting column (W) of the table. A combined decision can now be made using the weighting matrix together with the predicted class, using Equation 6 to judge the nature of the target. The result of this technique applied to the 20% validation data is shown in the combined decision row of Table 1.

| Node / Zone | 1 | | 2 | | 3 | | 4 | | 5 | | 6 | |
|-------------------|------|-------|------|-------|------|------|------|-------|------|------|------|-------|
| | S | W | S | W | S | W | S | W | S | W | S | W |
| 1 | 96.5 | 230.2 | 85.4 | 60.6 | 68.6 | 27.3 | 92.2 | 102.4 | 81.1 | 43.8 | 93.3 | 135.9 |
| 2 | 84.9 | 52.5 | 65.9 | 24.5 | 88.3 | 59.7 | 36.6 | 11.1 | 88.9 | 67.0 | 74.1 | 33.2 |
| 3 | 70.0 | 25.3 | 93.0 | 144.4 | 72.9 | 26.9 | 96.0 | 209.6 | 87.6 | 62.3 | 89.6 | 81.9 |
| Combined Decision | 99.6 | | 99.3 | | 98.4 | | 99.3 | | 99.7 | | 99.7 | |

Table 1. Classification Score (S / %), Weighting (W) & Combined Decision / %

6.2 Deep Neural Network

The number of samples available for each neural network was insufficient for training (200 samples of 0.5 s) and produced unsatisfactory results. Therefore the data set was augmented by injecting Gaussian noise of increasing variance into the spectrograms otherwise known as Additive White Gaussian Noise (AWGN) this resulted in the generation of 1800 additional samples for 0.5 s). However, as a consequence of using this method, the de-noising properties of the auto-encoder

are stressed upon much more as they must identify and distinguish the primary features of the target amongst additional noise and any irrelevant information.

After training the DNN, the weights of the first auto-encoder were visualised to reveal the features which maximally excited the hidden units within the network, as the first layer contains 1000 neurons only a small segment of the weights are shown; this is displayed in Figure 5. It can be seen that telling features such as the micro-Doppler ‘tails’ and part of the main Doppler signature are causing the most neural excitations in this layer, this directly correlates with the selection of the bandwidth and amplitude vectors in the feature based system.

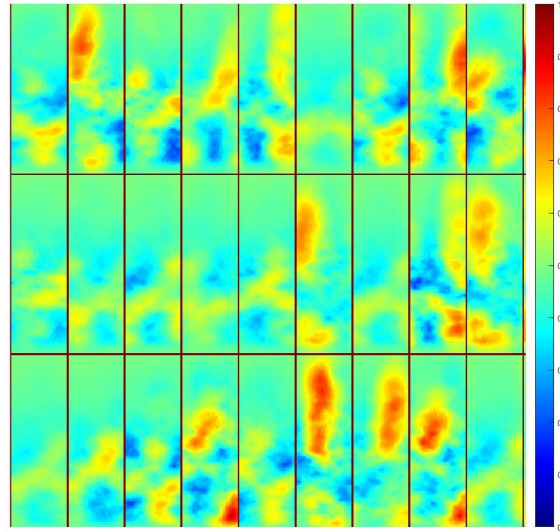


Fig. 5. Weights of the Auto-Encoder in the First Layer

Dwell Time - The relationship between dwell time and classification accuracy was explored, this is an interesting problem as reducing the dwell time can cause clashes with the average human walking gait and risks the misinterpretation of the target. The lower limit was found to be approximately 0.5 s, going lower than this meant that it was increasing likely for the ‘gaps’ in the swinging arm oscillations to be captured, this is disadvantageous as it is known that the most telling feature in this analysis is in fact the micro-Doppler peaks generated from the unconfined movements of the arm. On the other hand, increasing the dwell time allows for more information on the target to be captured, potentially allowing performance to be elevated; but doing so comes at the cost of the widening the input vector. Thus increasing the complexity of the NN and also, in a real time system, the length of time required before a judgement can be made. Three different dwell times were tested, being 0.5 s, 1 s, and 1.5 s and for each case a new set of neural networks were trained at 60% in exactly the same way as

the preceding section. The results are detailed in Table 2 with the minimum, maximum bounds showing the range of the node score.

| Classification Accuracy /% | | | | |
|----------------------------|---------|-------|---------|--------------------|
| Dwell /s | Minimum | Mean | Maximum | Std Dev / σ |
| 0.5 | 91.00 | 98.88 | 100.00 | 1.98 |
| 1.0 | 97.75 | 99.76 | 100.00 | 0.58 |
| 1.5 | 99.17 | 99.86 | 100.00 | 0.24 |

Table 2. Accuracy for varying Dwell Times

Unseen Person - To test the resilience of the trained network, data from another person operating in the field was applied (400 samples), this is an important test as each person has their own characteristic micro-Doppler signature and in a real situation the neural network would not have the luxury of training on prior data sets gathered from the person in question. This test will put particular emphasis on the generalisation performance of the network and its ability to recognise the important features rather than the specific patterns generated by the persons in which it trained on. The results of this analysis is shown in Table 3, for when the unseen person data is applied to the deep neural network (DNN) which is trained on 0.5 s dwell times at zone 5 in the field; data for Node 3 had to be held out due to an issue with recording.

| Zone 5 | Node 1 | Node 2 | Node 3 |
|-------------|--------|--------|--------|
| Accuracy /% | 70.5 | 99.1 | N/A |

Table 3. Accuracy for Unseen Person

Classification Ensembling with DNN - In this scenario the network has been trained at 60% for the 0.5 s case, 20% has been allocated for testing which generates the weighting matrix and the final 20% is used for validation. This process of sorting and applying the data is the same as the feed forward NN, allowing direct comparisons to be drawn; the results of this analysis are detailed in Table 4.

| Node / Zone | 1 | | 2 | | 3 | | 4 | | 5 | | 6 | |
|--------------------------|-------|-------|------|-------|------|-------|-------|-------|------|-------|-------|------|
| | S | W | S | W | S | W | S | W | S | W | S | W |
| 1 | 100.0 | 3000 | 98.8 | 270.0 | 98.8 | 159.3 | 99.8 | 497.5 | 99.8 | 492.5 | 100.0 | 3000 |
| 2 | 99.0 | 159.3 | 99.0 | 184.7 | 99.5 | 3000 | 98.5 | 184.6 | 99.5 | 3000 | 89.5 | 2.53 |
| 3 | 99.8 | 885.0 | 98.3 | 219.4 | 99.7 | 497.5 | 100.0 | 3000 | 99.3 | 350.3 | 100.0 | 3000 |
| Combined Decision | 100 | | 98.5 | | 99.5 | | 100 | | 100 | | 100 | |

Table 4. Classification Score (S / %), Weighting (W) & Combined Decision / %

Additional Tests - A comparative test was carried out to see how the configuration of stacked auto-encoders would perform when trained with samples from every zone and node rather than individually; producing one large neural network trained at 20% (7200 samples from a total of 36000). This was repeated 3 times and the average was taken, this resulted in a mean classification accuracy of 83.3 %.

7 Conclusions

This paper has presented the concept of classifying between unarmed vs potentially armed personnel using two different neural networks (NN). The former uses a two layer feed-forward NN pattern recognition algorithm, which accepts vectors extracted from a prior feature recognition algorithm. The latter uses a configuration of stacked auto-encoders, forming a DNN and then feeding spectrograms into this network directly, avoiding the extraction of handcrafted features through setting and tuning of thresholds. A form of weighted classification ensembling was proposed, which utilised prior information from evaluating the quality of each classifier to then decide the nature of the target using the predicted class across the three radar nodes to make a single decision. It has proved to be a powerful approach as it utilises all available information and is based on the principle that, even though a single network has good classification abilities, there is still the chance that it makes the wrong decision. The algorithm banks on this scenario as it gives the other nodes the opportunity to sway this decision if they believe that the superior node is wrong.

A distributed configuration was identified whereby unique neural networks were assigned to particular target locations in the field providing superior classification capabilities, this resulted in a 13.2% improvement for the DNN when implemented in this configuration over the de-centralised method. Further to this, the stacked auto-encoder approach resulted in an average node score of 98.9% compared to the feature based system score of 81.4%, an improvement of 17.5%. However when the feature based NN utilised the ensembled weighted decision algorithm it achieved an average overall accuracy of 99.3% and the stacked encoder scored 99.6%, demonstrating that the weighted decision particularly favours situations when the accuracy of single nodes in a system is inadequate. This was proven in the case of the unseen person, where Node 1 struggled, but Node 2 provided reliable results; applying the ensemble algorithm resulted in an overall accuracy of 99.6%. Further to this, the dwell time results indicated that longer is better but only by a marginal amount; however the standard deviation is shown to decrease noticeably as the dwell time increases which is certainly a desirable trait. In the scope of a real time system long dwell times would translate to overhead, not to mention the significant complexity introduced by using NN's trained to analyse much larger input matrices. In addition to this, the ensembling system can significantly enhance the results making this less of an issue, therefore it would be acceptable to implement the minimum dwell time of 0.5 s. The results obtained are comparable to that observed in prior literatures

(Fioranelli et al., 2016), where accuracies of approximately 98 % are reported, utilising a Naive Bayes classifier coupled with a binary voting algorithm.

The implication of these results is that it is ideal for NN's to analyse only an assigned area, as it proves to be difficult quantifying differences in the spectrogram ultimately arising from the range of angles to the target produced from the inherent geometry of a multistatic radar system. Modern radar systems work in real time and are provided with large sensor arrays coupled with high end hardware, so an handy expansion to this work would involve modifying the NNs to operate in real time environment and to take advantage of such systems. Such an improvement could lead to a NN based classifier which can continually train itself on human targets, adjusting its weights to ensure optimal classification whilst generating its own database of targets.

An investigation into a variety of situations in the field should also be considered to stress the systems further and to present a more realistic scenario for the radar: such as various body types, the target crawling, running or being hindered by carrying a large object (Youngwook & Moon, 2016). Another extension would involve increasing spatial variance and to test different deployment geometries of the radar sensors, adding greater variability to the bistatic and aspect angles considered. An emerging field of research is the concept of cognitive radar (Haykin, 2006), where there is the potential for an expansion in this system, whereby the NN develops a metric based on certain evaluations on the target. This would then be passed onto another layer in the radar system which decides what RF parameters it can adjust to allow an improvement in the quality of target, hence improving the classification abilities of the subsequent network.

References

1. Chen, V.C., Tahmoush, D., Miceli W.L. (2014) Radar Micro-Doppler Signatures: Processing and Applications. Institution of Engineering and Technology (IET)
2. Derham, T.E., Doughty, S., Woodbridge, K., and Baker, C.J. (2007) Design and Evaluation of a Low-Cost Multistatic Netted Radar System. IET Radar, Sonar & Navigation, vol. 1, no. 5, pp. 362-368
3. Doughty, S.R. (2007) Development and Performance Evaluation of a Multistatic Radar System, Ph.D.dissertation, University College London
4. Fioranelli, F., Ritchie, M., Griffiths, H. (2015) Multistatic Human Micro-Doppler Classification of Armed/Unarmed Personnel. IET Radar Sonar & Navigation, vol. 9, issue 7, pp. 857-865
5. Fioranelli, F., Ritchie, M., Griffiths, H. (2015) Aspect angle dependence and Multistatic data fusion for micro-Doppler classification of armed/unarmed personnel. IET Radar, Sonar & Navigation, vol. 9, issue 9, pp. 1231-1239
6. Fioranelli, F., Ritchie, M., Griffiths, H. (2016) Centroid features for classification of armed/unarmed multiple personnel using multistatic human micro-Doppler. IET Radar, Sonar & Navigation, vol. 10, no. 9, pp. 1702-1710, 12 2016.
7. Haykin, S. (2006) Cognitive Radar: A Way of the Future. IEEE Signal Processing Magazine, vol. 23, no. 1, pp. 30-40

8. Haykin, S. (2008). Neural Networks and Learning Machines: A Comprehensive Foundation. (3rd Edition), Pearson Prentice Hall
9. Jordan, T. S. (2016). Using convolutional neural networks for human activity classification on micro-Doppler radar spectrograms, Proceedings. SPIE, vol. 9825
10. Jokanovic, B., Amin, M., and Ahmad, F. (2016). Radar fall motion detection using deep learning, 2016 IEEE Radar Conference (RadarConf). pp. 16
11. Jokanovic, B., Amin, M., and Ahmad, F. (2016) Effect of data representations on deep learning in fall detection, IEEE Sensor Array and Multichannel Signal Processing Workshop (SAM). pp. 15
12. Jokanovic, B., Amin, M., and Erol, B. (2017) Multiple joint-variable domains recognition of human motion, 2017 IEEE Radar Conference, Seattle
13. Kwon, J., Kwak, N. (2017) Human detection by neural networks using a low-cost short-range Doppler radar sensor, 2017 IEEE Radar Conference, Seattle
14. Seyfioglu, M., Gurbuz, S., Ozbayoglu, A., Yuksel, M. (2017). Deep learning of micro-Doppler features for aided and unaided gait recognition. 2017 IEEE Radar Conference, Seattle
15. Stimson, G W., Griffiths, H D., Baker, C J., Adamy, D. (2014). Stimson's Introduction to Airborne Radar. (3rd Edition) SciTech (IET)
16. LeCun, Y., Bengio, Y., and Hinton, G. (2015). Deep learning, *Nature*, vol. 521, no. 7553, pp. 436-444
17. Park, J., Javier, R. J., Moon, T., and Kim, Y. (2016). Micro-Doppler Based Classification of Human Aquatic Activities via Transfer Learning of Convolutional Neural Networks, *Sensors*, vol. 16, no. 12, 2016.
18. Parashar, K., Ovemeke, M., Rykunov, M., Sahli, M., Bourdoux. (2017). A. Micro-Doppler feature extraction using convolutional auto-encoders for low latency classification, IEEE Radar Conference, Seattle
19. Tahmoush, D. and Silvious., J. (2009). Radar microDoppler for security applications: Modelling men versus women. IEEE Antennas and Propagation Society International Symposium, APSURSI, pp. 1-4, 1-5, Charleston, SC, USA.
20. Tahmoush, D. and J. Silvious. (2009). Remote detection of humans and animals. IEEE Applied Imagery Pattern Recognition Workshop (AIPRW), pp. 1-8, 14-16 October, Washington DC, USA.
21. Tivive, F., Bouzerdoum, A., Amin, M. (2010) A human gait classification method based on radar Doppler spectrograms. *EURASIP J. Adv. Signal Process*
22. Youngwook, K., Hao, L. (2008) Human activity classification based on micro-Doppler signatures using an artificial neural network. IEEE Antennas and Propagation Society International Symposium San Diego., pp 1-4
23. Youngwook, K., Hao, L. (2009) Human activity classification based on micro-Doppler signatures using a support vector machine. *IEEE Transactions on Geoscience and Remote Sensing*, vol.47, issue 5, pp. 1328-1337
24. Youngwook, K., Sungjae, H., Jihoon, K. (2015) Human detection using Doppler radar based on physical characteristics of targets. *IEEE Geoscience and Remote Sensing Letters*, vol. 12, issue 2, pp. 289-293.
25. Youngwook., K and Moon., T. (2016). Human Detection and Activity Classification Based on Micro-Doppler Signatures Using Deep Convolutional Neural Networks. *IEEE Geoscience and Remote Sensing Letters*, vol. 13, no. 1. pp. 8-12
26. Youngwook., K and Toomajian, B. (2016). Hand Gesture Recognition Using Micro-Doppler Signatures With Convolutional Neural Network, *IEEE Access*, vol. 4